

Entrainment of Central Pattern Generators to Natural Oscillations of Collocated Mechanical Systems

Y. Futakata and T. Iwasaki

Mechanical and Aerospace Engineering, University of Virginia
122 Engineer's Way, Charlottesville, VA 22904
Email: {futakata,iwasaki}@virginia.edu

Abstract—Rhythmic movements during animal locomotion are controlled by the neuronal circuits called central pattern generators (CPGs). The intrinsic frequency of a CPG in isolation is often different from that of observed movements, but appears to entrain to a natural mode of body oscillation through sensory feedback to achieve efficient locomotion. The objective of this paper is to reveal the feedback control mechanism underlying the entrainment of CPGs. Motivated by musculo-skeletal biomechanics, we consider the class of mechanical systems for which actuators, sensors, springs and dampers, are all collocated. Our main result provides a condition under which a CPG-based controller approximately achieves a selected mode of natural oscillation with a bound on the entrainment error.

I. INTRODUCTION

During animal locomotion, energy consumption appears to be minimized by exploiting the mechanical resonance inherent to the body and surrounding environment. The rhythmic body movement is controlled by the neuronal circuit called the central pattern generator (CPG) [1]. CPGs are biological oscillators activating the muscle contractions in a coordinated manner, where the commanded pattern is modified through sensory feedback in response to environmental changes.

A fundamental question is how the CPG processes the sensory information to achieve *natural entrainment*, i.e., to determine, and entrain to, the resonance frequency and corresponding natural motion. The problem has been addressed in the literature, but only for single degree-of-freedom (DOF) systems [2]–[5]. Through a study of a damped pendulum driven by a simple CPG, called the reciprocal inhibition oscillator (RIO) [6], *positive rate feedback* and *negative integral feedback* have been identified as a basic mechanism for resonance entrainment.

In this paper, we extend the analytical result in [5] for a class of n -DOF collocated mechanical systems. We consider distributed feedback controllers consisting of RIOs, each of which is placed between a pair of actuator and sensor, without direct communications to other RIOs. Conditions are obtained for the intrinsic RIO frequency and feedback gains such that a selected mode of natural oscillation is achieved for the closed-loop system. Our results are approximate in nature due to the limitation of the method employed, harmonic balancing. However, numerical simulations confirm reliability of our results. All proofs and preliminary lemmas are omitted due to the page limitation.

This work is supported by NSF0654070 and NSF0237708.

We use the following notation. For matrices A and B , $A \otimes B$ denotes the Kronecker product. For a vector $v \in \mathbb{R}^n$, $\text{diag}(v)$ denotes the $n \times n$ diagonal matrix whose (i, i) entry is the i^{th} entry of v . For a function f and a set X , the collection of $f(x)$ for various $x \in X$ is denoted by $f(X)$. The set of integers from 1 to n is denoted by \mathbb{I}_n .

II. PROBLEM FORMULATION

A. Reciprocal Inhibition Oscillator

We use the RIO as the basic control unit. The RIO is a simple CPG consisting of two neurons with mutually inhibitory synaptic connections as shown in Fig. 1, where $\mu > 0$ is the synaptic strength parameter and \mathcal{N} represents a neuron. The neuronal dynamics \mathcal{N} is modeled by the following mapping from the synaptic input w to the membrane potential (or spike frequency) v :

$$v = \psi(q), \quad q = b(s)w, \quad b(s) := \frac{2\omega_o s}{(s + \omega_o)^2},$$

where $\omega_o > 0$. We choose the band pass filter to embed the time lag and the adaptation effect, for the latter is essential for an RIO [6]. The static nonlinearity $\psi : \mathbb{R} \rightarrow \mathbb{R}$ is typically a sigmoid function and the following properties are assumed:

- ψ is odd, bounded, and strictly increasing.
- $\psi(x)$ is strictly concave on $x > 0$, and $\psi'(0) = 1$.

We denote by Ψ the class of functions satisfying these conditions. A function $\psi \in \Psi$ satisfies the slope condition

$$0 < \frac{\psi(x) - \psi(y)}{x - y} < 1,$$

for any $x \neq y$, and the slope is maximum at the origin as shown in [5]. For example, $\tanh(x)$ belongs to this class.

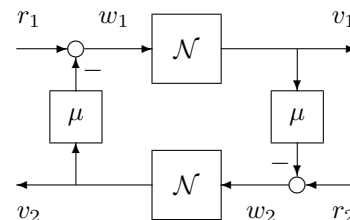


Fig. 1. Reciprocal inhibition oscillator

Following the development in [5], we consider the control unit in Fig. 2 where u and y are the activation input to,

and sensory output from, the mechanical system, and g and h are feedback gains. This architecture is motivated by the biological control mechanism where the neurons in the CPG receive sensory feedback, and the membrane potentials (or spike frequency) of the neurons are used for muscle activation.

The relation between y and u is described by

$$q = b(s)(M_o\Psi_o(q) + Hy), \quad u = G\Psi_o(q), \quad (1)$$

where

$$M_o := -\mu \begin{bmatrix} 0 & 1 \\ 1 & 0 \end{bmatrix}, \quad \Psi_o(q) := \begin{bmatrix} \psi(q_1) \\ \psi(q_2) \end{bmatrix}, \quad (2)$$

$$l := [1 \quad -1]^\top, \quad G := gl^\top, \quad H := hl.$$

The structure of H guarantees that the out-of-phase property of RIO oscillations is preserved and we have

$$\lim_{t \rightarrow \infty} |q_1(t) + q_2(t)| = 0,$$

for any initial states $q(0)$ and $\dot{q}(0)$ and arbitrary input y as shown in [5]. Moreover, with $y(t) \equiv 0$ and $\mu > 1$, the internal variables $q_1(t)$ and $q_2(t)$ in the RIO autonomously oscillate. It can be shown that the harmonic balance method predicts the frequency of the autonomous oscillation to be the center frequency ω_o of $b(s)$. For this reason we call ω_o the intrinsic frequency of the RIO.



Fig. 2. RIO-based control unit

B. Oscillation Analysis Problems

Consider the class of mechanical systems given by

$$J\ddot{x} + D\dot{x} + Kx = Bu, \quad y = Cx, \quad (3)$$

where $x(t) \in \mathbb{R}^n$, $u(t) \in \mathbb{R}^n$, and $y(t) \in \mathbb{R}^n$ are the generalized coordinates, inputs, and outputs, respectively.

Assumption 1: The system matrices J , D , and K are symmetric positive definite, B and C are square nonsingular, and, for positive scalars ρ and k_i with $i \in \mathbb{I}_n$, we have

$$C = B^\top, \quad D = \rho K,$$

$$K = BKC, \quad \mathcal{K} := \text{diag}(k_1, \dots, k_n).$$

Moreover, the natural frequencies are distinct.

The conditions in Assumption 1 are motivated by biological systems where the actuators, sensors, stiffness and damping elements are all located at the same position. In addition, Rayleigh damping $D = \rho K$ and distinct natural frequencies are assumed so that the analysis becomes simple enough to provide insights into the natural entrainment mechanism. We shall refer to the system (3) satisfying Assumption 1 as the *collocated system*.

We will develop a theory for the *linear* collocated system, but will examine, through numerical experiments, applicability of the theory to nonlinear systems whose linearized

system is given by (3). For later reference, let us recall that a natural mode of the system (3) is defined by a pair of the natural frequency $\omega_i \in \mathbb{R}_+$ and mode shape $x_i \in \mathbb{R}^n$ satisfying $(K - \omega_i^2 J)x_i = 0$ with $\|x_i\| = 1$. There are n natural modes, (ω_i, x_i) with $i \in \mathbb{I}_n$, for the n -DOF collocated system. Let us arrange the natural frequencies in the ascending order: $0 < \omega_1 < \omega_2 < \dots < \omega_n$.

CPGs often consist of multiple segmental oscillators that are coupled to each other. For undulatory swimming animals like leeches and lampreys, for instance, the CPG is formed as a chain of segmental oscillators, each of which receives local sensory feedback and induces local muscle contraction. The intersegmental coupling is considered essential for coordinating the phase timing of the oscillators so that traveling waves are generated down the slender body. However, experiments have shown that this is not true; even if the nerve cord connecting the segmental oscillators is severed in the middle of the body, the leech can still swim by coordinating the head and tail undulations based on the sensory feedback information [7].

Motivated by this result, we consider the extreme case where the collocated system is driven by n RIO-based control units (1) that are completely uncoupled to each other. In particular, each RIO drives an actuator and receives no direct signals from the other RIOs but only the local sensory feedback. The RIOs share the same intrinsic frequency ω_o and synaptic strength μ . Let $(g_i, h_i) \in \mathbb{R} \times \mathbb{R}$ and $q_i(t) \in \mathbb{R}^2$ be the feedback gains and internal variable for the i^{th} unit. The set of n units can be written as

$$q = b(s)(M\Psi(q) + Hy), \quad u = G\Psi(q) \quad (4)$$

where

$$M := I \otimes M_o, \quad G := \text{diag}(g) \otimes l^\top, \quad H := \text{diag}(h) \otimes l,$$

$$g := [g_1 \quad \dots \quad g_n]^\top, \quad h := [h_1 \quad \dots \quad h_n]^\top,$$

$$q := \begin{bmatrix} q_1 \\ \vdots \\ q_n \end{bmatrix}, \quad \Psi(q) := \begin{bmatrix} \Psi_o(q_1) \\ \vdots \\ \Psi_o(q_n) \end{bmatrix}.$$

The closed-loop system consisting of the linearized mechanical system (3) and the CPG-based controller (4) is described by the kernel representation:

$$Z(s, \Psi)\xi = 0, \quad \xi := \begin{bmatrix} x \\ q \end{bmatrix}, \quad (5)$$

$$Z(s, \Psi) := \begin{bmatrix} Js^2 + Ds + K & -BG\Psi \\ b(s)HC & b(s)M\Psi - I \end{bmatrix}. \quad (6)$$

We address the following problems posed on (5):

- 1) Characterize the relationship between the oscillation profile and the parameters of the plant (3) and controller (4) for the closed-loop system (5).
- 2) Determine a condition under which the natural entrainment is approximately induced and quantify the closeness to the specified natural frequency.
- 3) Prove that the derived condition for the natural entrainment guarantees that ξ oscillates in the steady state.

Since we are interested in natural entrainment, we will restrict our attention to the oscillations with one of the natural mode shapes. The answers for 1), 2) and 3) will be given by Theorems 1, 2 and 3, respectively.

III. APPROACH VIA HARMONIC BALANCE

A. Multivariable Harmonic Balance Method

Assume that (5) has a periodic solution $\xi(t)$ with frequency ω . We shall approximate $\xi(t)$ by sinusoidal signals and ψ by its describing function κ defined by

$$\kappa(\alpha) := \frac{4}{\alpha\pi} \int_0^{\pi/2} \psi(\alpha \sin \theta) \sin \theta d\theta. \quad (7)$$

It was shown in [5] that $\kappa(\alpha)$ for $\psi \in \Psi$ takes a value in the interval $(0, 1)$ when $\alpha > 0$, and κ is strictly decreasing from 1 to 0 as $\alpha > 0$.

Let $\hat{\xi}$ be the phasor of $\xi(t)$ and partition it into $\hat{x} \in \mathbb{C}^n$ and $\hat{q} \in \mathbb{C}^{2n}$. The MHB equation for (5) is given by

$$Z(j\omega, \Phi)\hat{\xi} = 0, \quad (8)$$

$$\hat{q} := \hat{\alpha} \otimes I, \quad \Phi := \text{diag}(\kappa(|\hat{\alpha}_1|), \dots, \kappa(|\hat{\alpha}_n|)) \otimes I.$$

The structure of \hat{q} is enforced without loss of generality due to the structure of H [5]. Let us define the associated linear system by

$$Z(s, \Phi)\xi = 0. \quad (9)$$

The basic idea of the MHB method is the following.

- If the MHB equation (8) is satisfied, then the system (5) is expected to possess the oscillatory trajectory

$$\begin{aligned} x_i(t) &\cong |\hat{x}_i| \sin(\omega t + \theta_i), \\ q_i(t) &\cong \begin{bmatrix} |\hat{\alpha}_i| \sin(\omega t + \phi_i) \\ -|\hat{\alpha}_i| \sin(\omega t + \phi_i) \end{bmatrix}, \end{aligned}$$

where $\theta_i := \angle \hat{x}_i$, and $\phi_i := \angle \hat{\alpha}_i$ for $i \in \mathbb{I}_n$.

- If the associated linear system (9) is marginally stable for the amplitude $|\hat{\alpha}_i|$ predicted from (8), then the estimated oscillation is expected to be stable.

For given mechanical system (J, D, K, B, C) and controller (ω_o, μ, g, h) and $\psi \in \Psi$, we call $(\omega, \hat{x}, \hat{\alpha})$ a *stable solution* of (8) if it satisfies (8) and (9) is marginally stable.

B. Basic Analysis

The MHB equation (8) provides an estimated relationship between the system parameters and the resulting oscillation profile. Since we are interested in natural entrainment, we consider the case where $x(t)$ oscillates with one of the natural mode shapes, but its frequency ω is not fixed to the natural frequency to allow for perturbation analysis. With $\hat{x} := x_\ell$ for a selected $\ell \in \mathbb{I}_n$, the MHB equation reduces to more insightful conditions. To present the result, define, for $i \in \mathbb{I}_n$,

$$\varpi_o := \frac{1}{2} \left(\frac{\omega}{\omega_o} - \frac{\omega_o}{\omega} \right), \quad \varpi_i := \frac{1}{2} \left(\frac{\omega}{\omega_i} - \frac{\omega_i}{\omega} \right), \quad (10)$$

$$\zeta_i := \frac{\omega_i}{2} \rho, \quad \gamma_i := (\mu - 1)\zeta_i, \quad (11)$$

$$f_i(\omega) := \varpi_o \varpi_i, \quad g_i(\omega) := \frac{\omega \varpi_o (\varpi_i^2 + \zeta_i^2)}{\omega_i (\varpi_o \varpi_i - \zeta_i)}. \quad (12)$$

Theorem 1: Let the plant (3) and controller (4) be given, where $\psi \in \Psi$ and Assumption 1 holds. Let $\omega \in \mathbb{R}_+$, $\hat{\alpha} \in \mathbb{C}^n$, and $\ell \in \mathbb{I}_n$ be given. Suppose $g_i h_i \hat{\alpha}_i \neq 0$ for all $i \in \mathbb{I}_n$. Then the MHB equation (8) with $\hat{x} := x_\ell$ is satisfied if and only if there exist $\eta \in \mathbb{R}$ and $a \in \mathbb{R}_+$ such that

$$\kappa(a) = \frac{1}{\mu} \left(1 - \frac{f_\ell(\omega)}{\zeta_\ell} \right), \quad (13)$$

$$g_\ell(\omega) = \frac{\eta}{\mu}, \quad (14)$$

$$\begin{aligned} \frac{h_i \hat{y}_i}{\hat{\alpha}_i} &= \frac{\varpi_o}{\zeta_\ell} (\varpi_\ell + j\zeta_\ell), \\ |\hat{\alpha}_i| &= a, \quad g_i h_i = k_i \eta, \end{aligned} \quad (15)$$

for all $i \in \mathbb{I}_n$ where κ is defined by (7), and \hat{y}_i is the i^{th} entry of $\hat{y} := C\hat{x}$. In this case, it holds that

$$-\gamma_\ell < f_\ell(\omega) < \zeta_\ell, \quad (16)$$

and (9) has poles at $s = \pm j\omega$.

Furthermore, all the poles of (9) except $s = \pm j\omega$ are in the open left half plane if and only if

$$-\min(\beta, v_i) < f_\ell(\omega), \quad (17)$$

$$g_i(w_i^+) < g_\ell(\omega) < g_i(w_i^-), \quad (18)$$

for all $i \neq \ell$, $i \in \mathbb{I}_n$, where ζ_i , f_i and g_i are defined by (11) and (12), $w = w_i^\pm$ are the unique positive solutions of $\omega_\ell f_i(w) = \omega_i f_\ell(\omega)$ with $w_i^- < w_i^+$, and

$$\beta := \frac{(\rho\omega_1)^2 \omega_\ell}{4\omega_o}, \quad v_i := \frac{\omega_\ell}{4\omega_i} \left(\sqrt{\frac{\omega_o}{\omega_i}} - \sqrt{\frac{\omega_i}{\omega_o}} \right)^2. \quad (19)$$

The result indicates that, for the closed-loop system (5) to oscillate with the natural mode shape x_ℓ , it is necessary that (i) the magnitudes of the sensory feedback, $|h_i \hat{y}_i|$, are uniform over all RIOs (or $i \in \mathbb{I}_n$), and (ii) the overall feedback gain, $g_i h_i$, is proportional to the stiffness (or damping) of the input/output channel k_i (or ρk_i). The assumption $g_i h_i \hat{\alpha}_i \neq 0$ is reasonable because it implies that all the control inputs are used ($g_i \neq 0$), every RIO receives sensory feedback ($h_i \neq 0$) and oscillates ($\hat{\alpha}_i \neq 0$).

Another observation from Theorem 1 is that, whenever $x(t)$ oscillates with the natural mode shape x_ℓ and the oscillation is stable, its frequency ω is expected to be in \mathcal{W}_ℓ which is defined as the set of ω satisfying (16)–(18) for all $i \neq \ell$, $i \in \mathbb{I}_n$. Conversely, if the gains are chosen such that $\eta/\mu \in g_\ell(\mathcal{W}_\ell)$ and the uniformity and proportionality conditions are satisfied, then there is a stable solution $(\omega, x_\ell, \hat{\alpha})$ to the MHB equation, predicting the existence of a stable oscillation with frequency $\omega \in \mathcal{W}_\ell$ as summarized below.

Corollary 1: Let the plant (3) and controller (4) be given, where $\psi \in \Psi$ and Assumption 1 holds. Let $\ell \in \mathbb{I}_n$ be given and \hat{y}_i be the i^{th} entry of $\hat{y} := Cx_\ell$. Suppose there exist $\eta \in \mathbb{R}$ and $r_o > 0$ such that

$$g_i h_i = k_i \eta, \quad |h_i \hat{y}_i| = r_o \quad \forall i \in \mathbb{I}_n, \quad (20)$$

and $\eta/\mu \in g_\ell(\mathcal{W}_\ell)$. Then the MHB equation (8) has a stable solution $(\omega, \hat{x}, \hat{\alpha})$ where

$$\hat{x} = \sigma x_\ell, \quad \hat{\alpha}_i = \text{sgn}(h_i \hat{y}_i \varpi_o) a e^{j\phi}, \quad (21)$$

$$\sigma := \frac{a}{r_o} \left| \frac{\varpi_o}{\sin \phi} \right|, \quad \phi := \angle(\varpi_\ell - j\zeta_\ell). \quad (22)$$

and (ω, a) is a solution of (13) and (14).

While this result predicts existence and profile of oscillations for a given set of feedback gains, one can reverse the process to develop design equations. That is, one can obtain explicit formulas for the feedback gains (g, h) that would achieve a stable oscillation for the collocated system with a prescribed frequency ω , amplitude σ , and natural mode shape x_ℓ , i.e., $x(t) \cong \sigma x_\ell \sin \omega t$.

Corollary 2: Let the plant (3) and controller (4) be given, where $\psi \in \Psi$ and Assumption 1 holds. Let $\ell \in \mathbb{I}_n$, $\sigma > 0$, and $\omega \in \mathcal{W}_\ell$ be given. Then there exists $\hat{\alpha} \in \mathbb{C}^n$ such that $(\omega, \sigma x_\ell, \hat{\alpha})$ is a stable solution of (8) if feedback gains (g, h) are given by

$$g_i = \frac{k_i \mu g_\ell(\omega)}{h_i}, \quad h_i = -\frac{\varpi_o a |\varpi_\ell + j\zeta_\ell|}{\sigma \zeta_\ell |\hat{y}_i|}, \quad (23)$$

where \hat{y}_i is the i^{th} entry of $\hat{y} := Cx_\ell$, and a is the solution of (13).

IV. MAIN RESULTS

A. Mechanism of Natural Entrainment

We have seen in Corollary 1 that a stable oscillation with the natural mode shape x_ℓ is expected if the gains satisfy the uniformity and proportionality conditions and $\eta/\mu \in g_\ell(\mathcal{W}_\ell)$. A drawback of this result is that the characterization of the gain set $g_\ell(\mathcal{W}_\ell)$ is complex and does not indicate the structure of the set (e.g., a few intervals or many intervals). Moreover, it is not clear what subset of the gain set yields stable oscillations with frequencies close to the natural frequency ω_ℓ . This section will address these issues.

To this end, we consider a subset of gains $g_\ell(\mathcal{W}_\ell)$ which admits a simple and clean characterization. In particular, we consider $g_\ell(\tilde{\mathcal{W}}_\ell)$ where $\tilde{\mathcal{W}}_\ell := \mathcal{V}_\ell \cap \mathcal{W}_\ell$ with

$$\mathcal{V}_\ell := \{\omega \in \mathbb{R}_+ \mid -\min(\gamma_\ell, 0) < f_\ell(\omega) < \zeta_\ell\}. \quad (24)$$

Using the property of g_ℓ , the set $g_\ell(\mathcal{V}_\ell)$ can be explicitly characterized as

$$g_\ell(\mathcal{V}_\ell) = \{x \in \mathbb{R} \mid x < g_\ell(\omega_m) \text{ or } g_\ell(\omega_m) < x\}, \quad (25)$$

$$\omega_m := \min(\omega_o, \omega_\ell, \omega_\gamma^-), \quad \omega_M := \max(\omega_o, \omega_\ell, \omega_\gamma^+), \quad (26)$$

where $\omega = \omega_\gamma^\pm$ are the positive solutions of $f_\ell(\omega) = -\gamma_\ell$ with $\omega_\gamma^- \leq \omega_\gamma^+$ if they exist; otherwise let $\omega_\gamma^\pm := \mp\infty$.

Now, it can be shown that $\eta/\mu \in g_\ell(\tilde{\mathcal{W}}_\ell)$ holds if and only if $\eta/\mu \in g_\ell(\mathcal{V}_\ell)$ and $a_\ell > a_i$ hold for all $i \neq \ell$, $i \in \mathbb{I}_n$, where a_1, \dots, a_n are defined for η/μ as follows.

Definition 1: For given $i \in \mathbb{I}_n$ and $\eta/\mu \in \mathbb{R}$, set $a_i := 0$ if $\eta/\mu \notin g_i(\mathcal{V}_i)$; otherwise, let ω be the positive solution $\omega \in \mathcal{V}_i$ to (14) with $\ell = i$, and define a_i as the solution a to (13) with $\ell = i$

The existence and uniqueness of ω and a_i in the above definition are guaranteed by $\eta/\mu \in g_i(\mathcal{V}_i)$ [5]. We are now ready to state a main result.

Theorem 2: Let the plant (3) and controller (4) be given, where $\psi \in \Psi$ and Assumption 1 holds. Suppose there exists $\eta \in \mathbb{R}$ such that $g_i h_i = k_i \eta$ for all $i \in \mathbb{I}_n$. Let a_i for $i \in \mathbb{I}_n$ be as specified in Definition 1 and let $\ell \in \mathbb{I}_n$ be such that $a_\ell > a_i$ for all $i \neq \ell$, $i \in \mathbb{I}_n$. Furthermore, suppose $\eta/\mu \in g_\ell(\mathcal{V}_\ell)$ and there exists $r_o > 0$ such that $|h_i \hat{y}_i| = r_o$ for all $i \in \mathbb{I}_n$ where \hat{y}_i is the i^{th} entry of $\hat{y} := Cx_\ell$.

Then, a stable solution of (8) is given by $(\omega, \hat{x}, \hat{\alpha})$ where $\omega \in \mathcal{V}_\ell$ is the solution to (14) and \hat{x} and $\hat{\alpha}$ are specified by (21), (22), and (13). Furthermore, the frequency ω satisfies the following:

- ω is close to $\omega_* := \min(\omega_o, \omega_\ell)$ if $\eta/\mu > g_\ell(\omega_m)$.
- ω is close to $\omega_* := \max(\omega_o, \omega_\ell)$ if $\eta/\mu < g_\ell(\omega_m)$,

where the closeness is in the sense that

$$\left| \frac{\omega - \omega_*}{\omega_*} \right| \leq \left| \frac{\zeta_\ell}{\varpi} \right|, \quad \varpi := \frac{1}{2} \left(\frac{\omega_o}{\omega_\ell} - \frac{\omega_\ell}{\omega_o} \right). \quad (27)$$

Theorem 2 provides a characterization of the feedback gains η/μ such that the closed-loop system is expected to oscillate with a natural mode shape. Furthermore, it shows that the frequency of oscillation would be close to either the intrinsic RIO frequency ω_o or the natural frequency ω_ℓ , with an explicit bound on the frequency perturbation (27). The bound gets smaller as the damping ζ_ℓ gets smaller and/or the difference between ω_o and ω_ℓ gets larger. This is in agreement with the case of one-DOF systems [5].

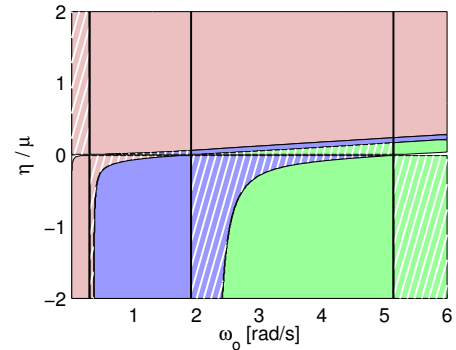


Fig. 3. An example of mode partitions ($\omega_1 = 0.292$, $\omega_2 = 1.92$, $\omega_3 = 5.15$); solid pink: (1, 1), shaded pink: (0, 1), solid blue: (2, 2), shaded blue: (0, 2), solid green: (3, 3), shaded green: (0, 3), where in the region labeled as (p, q) , the MHB analysis predicts that the closed-loop oscillation has a frequency close to the p^{th} natural frequency ω_p (or the intrinsic RIO frequency if $p = 0$) with the q^{th} natural mode shape x_q .

Consider the control design problem of achieving a closed-loop oscillation with a natural mode shape. The essential degree of freedom of the controller parameters (ω_o, μ, g, h) is only two and represented by $(\omega_o, \eta/\mu)$ due to the uniformity and proportionality requirements on the gains as seen in Theorem 1. For a given pair $(\omega_o, \eta/\mu)$, one can determine which mode of natural oscillations is expected stable by examining whether $a_\ell > a_i$ for all $i \neq \ell$, $i \in \mathbb{I}_n$ as shown in Theorem 2. As a result, one can draw partitions on the

$(\omega_o, \eta/\mu)$ -plane so that in each partitioned region a distinct pair of frequency and natural mode shape is achieved.

Figure 3 shows an example of the mode-partition diagram for a 3-link mechanical system. Each colored area represents the entrained frequency and natural mode shape, and the thick vertical lines represent the natural frequencies. The entrained frequency in the solid area is close to ω_ℓ while that in the shaded area is close to ω_o in the sense of (27). For example, the solid blue region (2,2) implies that the oscillation shape is the second mode and ω is close to ω_2 while the shaded blue region (0,2) implies that the oscillation shape is the second mode but ω is close to ω_o .

B. Existence of Stable Oscillations

We now turn our attention to the condition for existence of oscillation. The MHB method in Theorem 2 predicts that the closed-loop system (5) has a stable oscillatory trajectory when the feedback gains satisfy the uniformity and proportionality conditions (20) and $\eta/\mu \in g_\ell(\mathcal{V}_\ell)$ for the particular ℓ specified by the property $a_\ell > a_i$. Since the MHB analysis is based on sinusoidal approximations, the result does not rigorously prove that the gain conditions guarantee the existence of oscillations. It turns out, however, that the conditions are indeed sufficient to guarantee existence of oscillations. In fact, the conditions can be relaxed to the requirements that $g_i h_i = k_i \eta$ for all $i \in \mathbb{I}_n$ and $\eta/\mu \in g_\ell(\mathcal{V}_\ell)$ for some $\ell \in \mathbb{I}_n$.

Theorem 3: Let the plant (3) and controller (4) be given, where $\psi \in \Psi$ and Assumption 1 holds. Suppose the origin of the closed-loop system (5) is a hyperbolic equilibrium, and there exist $\eta \in \mathbb{R}$ such that $g_i h_i = k_i \eta$ holds for all $i \in \mathbb{I}_n$, and $\eta/\mu \in \mathcal{G}$ where, with $g_\ell(\mathcal{V}_\ell)$ defined by (25),

$$\mathcal{G} := \bigcup_{\ell=1}^n g_\ell(\mathcal{V}_\ell). \quad (28)$$

Then, for almost all initial conditions, the trajectory $\xi(t)$ of (5) oscillates in the steady state.

The idea behind this result is the following. Using the fact that ψ is bounded, and $b(s)$ and plant (3) are stable, it can be shown that every trajectory is bounded. Due to $\psi(0) = 0$ and $b(0) = 0$, the origin $\xi = 0$ is the unique equilibrium of (5). Hence, if the origin is hyperbolic and unstable, then a generic trajectory cannot converge to a fixed point, nor diverge to infinity, resulting in oscillation in the sense of Yakubovich [8], [9]. When $\eta/\mu \in \mathcal{G}$ and $g_i h_i = k_i \eta$ for all $i \in \mathbb{I}_n$, the origin can be shown to be hyperbolic and unstable, and thus trajectories with almost all initial conditions oscillate. Note that the uniformity condition $|h_i \bar{y}_i| = r_o$ for all $i \in \mathbb{I}_n$ in Theorem 2 is not required to guarantee hyperbolic instability.

V. NUMERICAL EXPERIMENTS

Consider a flexible mechanical arm formed as a chain of three rigid links connected by two rotational joints to each other. The i^{th} link has mass m_i and length $2l_i$, and the first link is connected to the inertial frame through a rotational joint. Mounted at the i^{th} joint are a spring of stiffness k_i ,

a dashpot of damping coefficient ρk_i , and an actuator that generate torque input u_i . The equation of motion is given by

$$J_x \ddot{x} + G_x \dot{x}^2 + D \dot{x} + Kx = Bu, \quad y = Cx, \quad (29)$$

where x_i is the angular displacement of the i^{th} link, y_i is the relative angle between the i^{th} and $(i+1)^{\text{th}}$ links, \dot{x}^2 is the vector whose i^{th} entry is \dot{x}_i^2 , and

$$\begin{aligned} J_x &:= J_o + S_x Q S_x + C_x Q C_x, & G_x &:= S_x Q C_x - C_x Q S_x, \\ Q &:= L^T M L, & C &:= B^T, & K &:= B K C, & D &:= \rho K, \\ \mathcal{M} &:= \text{diag}(m_1, m_2, m_3), & \mathcal{K} &:= \text{diag}(k_1, k_2, k_3), \\ B &:= \begin{bmatrix} 1 & -1 & 0 \\ 0 & 1 & -1 \\ 0 & 0 & 1 \end{bmatrix}, & L &:= \begin{bmatrix} l_1 & 0 & 0 \\ 2l_1 & l_2 & 0 \\ 2l_1 & 2l_2 & l_3 \end{bmatrix}, \\ J_o &:= \text{diag}(m_1 l_1^2, m_2 l_2^2, m_3 l_3^2) / 3, \\ S_x &:= \text{diag}(\sin(x_1), \sin(x_2), \sin(x_3)), \\ C_x &:= \text{diag}(\cos(x_1), \cos(x_2), \cos(x_3)). \end{aligned}$$

We use the following parameter values:

$$l_i = 0.5, \quad m_i = 1.0, \quad k_i = 1.0, \quad \rho = 0.1,$$

for $i \in \mathbb{I}_3$. By linearizing (29) around the origin, we obtain (3) with $J := J_o + Q$. The natural frequencies and mode shapes are given by

	1 st mode	2 nd mode	3 rd mode
ω_ℓ	0.292	1.92	5.15
x_ℓ	0.402	0.476	0.291
	0.615	-0.242	-0.654
	0.678	-0.846	0.698

The mode-partition diagram for the link system are given by Fig. 3. Based on this figure, we selected the controller parameters $(\omega_o, \eta/\mu)$ as (A), (B) and (C) in the table below so that the entrained oscillation profiles are close to the 1st, 2nd and 3rd natural mode, respectively. For each case, we have designed the feedback gains (g, h) by (23), where $\mu = 1.5$ and $\psi(x) = \tanh(x)$.

	(A)	(B)	(C)
$(\omega_o, \eta/\mu)$	(0.2, -1.0)	(0.5, -1.0)	(3.0, -1.0)

First, to evaluate the accuracy of the MHB method, the linearized three-link chain system (3) was numerically simulated and we found the following results:

	ω_{MHB}	ω_{SIM}	e_{PRD}	e_ω	e_x	$ \zeta_\ell/\varpi $
(A)	0.302	0.302	0.077	3.28	0	3.76
(B)	1.99	1.99	0.197	3.88	0.276	5.37
(C)	6.25	6.17	1.18	20.0	4.34	45.4

where ω_{MHB} is the estimated frequency, $(\omega_{\text{NAT}}, x_{\text{NAT}})$ is the natural mode for which the controller was designed, $(\omega_{\text{SIM}}, x_{\text{SIM}})$ is the steady-state oscillation profile obtained by the simulations, and

$$\begin{aligned} e_{\text{PRD}} &:= \frac{|\omega_{\text{MHB}} - \omega_{\text{SIM}}|}{\omega_{\text{SIM}}} \times 100, & e_\omega &:= \frac{|\omega_{\text{SIM}} - \omega_{\text{NAT}}|}{\omega_{\text{NAT}}} \times 100, \\ e_x &:= \frac{\|\bar{x}_{\text{SIM}} - x_{\text{NAT}}\|}{\|x_{\text{NAT}}\|} \times 100, & \bar{x}_{\text{SIM}} &:= \frac{x_{\text{SIM}}}{\|x_{\text{SIM}}\|}. \end{aligned}$$

Thus, e_{PRD} measures the accuracy of prediction, and e_ω and e_x indicate the closeness of the entrained oscillation profile

to the natural mode. Since e_{PRD} and e_x are small, and e_ω is smaller than $|\zeta_e/\omega|$, we conclude that the MHB method provided fairly accurate result.

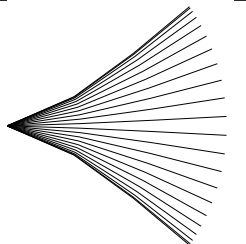
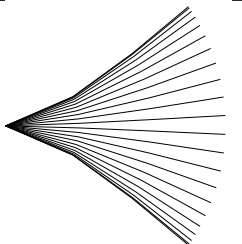
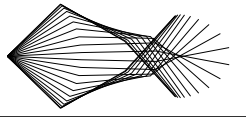
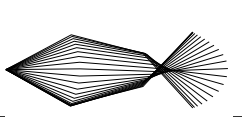


Next, we simulated the original system (29) with (g, h) designed above to evaluate applicability of the MHB method for nonlinear systems. Snapshots of the steady-state oscillation during a half period are depicted in the right column of Table I, and the frequencies ω_{SIM} are given by

	(A)	(B)	(C)
ω_{SIM}	0.303	1.58	3.98
ω_{NAT}	0.293	1.30	2.77

To evaluate whether the achieved steady-state oscillations are close to the corresponding natural modes of the nonlinear system (29), we have numerically determined the nonlinear natural modes as follows. Let the damping and input be zero ($\rho := 0$ and $u := 0$) in (29) and set the initial values so that the angular velocities are zero and the 3rd angle of (29) is equal to the simulated amplitude of $x_3(t)$. Then the initial values of the other angles $x_1(t)$ and $x_2(t)$ were searched by “fminsearch” in Matlab so that the square sum of the differences between the state values after one cycle and their initial values is minimized. The nonlinear natural modes are thus found through numerical computation, and the natural frequencies ω_{NAT} are given in the table above while the mode shapes are depicted in the left column of Table I. Although ω_{SIM} is not very close to ω_{NAT} for (B) and (C), the oscillation shapes in Table I are similar. Thus, we conclude that the RIO-based decentralized controller roughly achieved natural entrainment for the nonlinear system.

TABLE I

NONLINEAR NATURAL MODE SHAPES AND ACHIEVED OSCILLATIONS

	Nonlinear Natural Modes	Simulation Results
(A)		
(B)		
(C)		

VI. CONCLUSION

We have considered the feedback control system consisting of a collocated mechanical system (3) and distributed RIOs (4), and examined the natural entrainment condition under which the closed-loop system (5) oscillates at (or near) one of the natural modes of the mechanical system. Our findings can be summarized as follows.

- (i) If the closed-loop oscillations are desired to have one of the natural mode shapes, it is necessary for the feedback gains to satisfy (20), i.e., the overall gain for each input/output channel is proportional to the stiffness (or damping), and the magnitudes of the inputs to RIOs are uniform (Theorem 1).
- (ii) When the gains satisfy (20), the closed-loop system oscillates for almost all initial conditions if the feedback gains are sufficiently large in magnitude; $\eta/\mu \in \mathcal{G}$ (Theorem 3). For the rest of the statements, the gains are assumed to satisfy (20) and $\eta/\mu \in \mathcal{G}$.
- (iii) There may be multiple (up to n) solutions to the MHB equation (8), and among these, the oscillation with the largest amplitude is the one that is stable (Theorem 2).
- (iv) With positive feedback $\eta/\mu > 0$ and $\omega_1 < \omega_o$, the closed-loop oscillations are entrained to the first natural mode. With negative feedback $\eta/\mu < 0$ and $\omega_{i-1} \ll \omega_o < \omega_i$, the closed-loop oscillations are entrained to the i^{th} natural mode, where the lower bound on ω_o is replaced by zero when $i = 1$ (Fig. 3).
- (v) During the natural entrainment in item (iv), the error between the frequency of the closed-loop oscillation and the natural frequency is smaller if the distance between the intrinsic RIO frequency and the natural frequency is larger and/or the damping is small (Theorem 2).

Item (ii) is a result guaranteed by a rigorous proof, while the others are approximate results, derived from the MHB analysis, that are expected to hold if the oscillations are close to sinusoids. Numerical experiments have demonstrated that the approximate results are fairly reliable, even when applied to nonlinear collocated systems.

REFERENCES

- [1] S. Grillner, J.T. Buchanan, P. Walker, and L. Brodin. *Neural Control of Rhythmic Movements in Vertebrates*. New York: Wiley, 1988.
- [2] T. Iwasaki and M. Zheng. Sensory feedback mechanism underlying entrainment of central pattern generator to mechanical resonance. *Biological Cybernetics*, 94(4):245–261, 2006.
- [3] B.W. Verdaasdonk, H.F. Koopman, and F.C. Van der Helm. Resonance tuning in a neuro-musculo-skeletal model of the forearm. *Biological Cybernetics*, 96(2):165–180, 2007.
- [4] C.A. Williams and S.P. DeWeerth. A comparison of resonance tuning with positive versus negative sensory feedback. *Biol. Cyb.*, 96:603–614, 2007.
- [5] Y. Futakata and T. Iwasaki. Formal analysis of resonance entrainment by central pattern generator. *J. Math. Biol.*, 57(2):183–207, 2008.
- [6] W.O. Friesen. Reciprocal inhibition: A mechanism underlying oscillatory animal movements. *Neurosci. and Biobehav. Rev.*, 18(4):547–553, 1994.
- [7] X. Yu, B. Nguyen, and W. O. Friesen. Sensory feedback can coordinate the swimming activity of the leech. *J. Neurosci.*, 19(11):4634–4643, 1999.
- [8] V.A. Yakubovich. Frequency-domain criteria for oscillation in nonlinear systems with one stationary nonlinear component. *Siberian Mathematical Journal*, 14(5):768–788, 1973.
- [9] A. Pogromsky, T. Glad, and H. Nijmeijer. On diffusion driven oscillations in coupled dynamical systems. *Int. J. Bifurcation and Chaos*, 9(4):629–644, 1999.